



HAL
open science

Multi objective H_∞ active anti-roll bar control for heavy vehicles

van Tan Vu, Olivier Sename, Luc Dugard, Peter Gáspár

► To cite this version:

van Tan Vu, Olivier Sename, Luc Dugard, Peter Gáspár. Multi objective H_∞ active anti-roll bar control for heavy vehicles. IFAC WC 2017 - 20th IFAC World Congress, Jul 2017, Toulouse, France. pp. 13802 - 13807. hal-01394358

HAL Id: hal-01394358

<https://hal.science/hal-01394358v1>

Submitted on 9 Nov 2016

HAL is a multi-disciplinary open access archive for the deposit and dissemination of scientific research documents, whether they are published or not. The documents may come from teaching and research institutions in France or abroad, or from public or private research centers.

L'archive ouverte pluridisciplinaire **HAL**, est destinée au dépôt et à la diffusion de documents scientifiques de niveau recherche, publiés ou non, émanant des établissements d'enseignement et de recherche français ou étrangers, des laboratoires publics ou privés.

Multi objective H_∞ active anti-roll bar control for heavy vehicles

Van-Tan Vu* Olivier Sename* Luc Dugard* Peter Gaspar**

* Univ. Grenoble Alpes, CNRS, GIPSA-lab, F-38000 Grenoble, France.
E-mail: {Van-Tan.Vu, olivier.sename, luc.dugard}@gipsa-lab.grenoble-inp.fr
** Systems and Control Laboratory, Institute for Computer Science and Control, Hungarian Academy of Sciences, Kende u. 13-17, H-1111 Budapest, Hungary. E-mail: gaspar@sztaki.mta.hu

Abstract: In the active anti-roll bar control on heavy vehicles, roll stability and energy consumption of actuators are two essential but conflicting performance objectives. In a previous work, the authors proposed an integrated model, including four electronic servo-valve hydraulic actuators in a linear yaw-roll model on a single unit heavy vehicle. This paper aims to design an H_∞ active anti-roll bar control and solves a Multi-Criteria Optimization (MCO) problem by using Genetic Algorithms (GAs) to select the weighting functions for the H_∞ synthesis. Thanks to GAs, the roll stability and the energy consumption are handled using a single high level parameter and illustrated via the Pareto optimality. Simulation results in frequency and time domains emphasize the efficiency of the use of the GAs method for a MCO problem in H_∞ active anti-roll bar control on heavy vehicles.

Keywords: Active anti-roll bar, H_∞ control, Multi-criteria optimization, Genetic algorithms.

1. INTRODUCTION

The aim of rollover prevention is to provide the vehicle with the ability to resist overturning moments generated during vehicle maneuvers. Roll stability is determined by the height of the center of mass, the track width and the kinematic properties of the suspension. The primary overturning moment arises from the lateral acceleration acting on the center of gravity of the vehicle. More destabilizing moment arises during the cornering manoeuvre when the center of gravity of the vehicle shifts laterally. The roll stability of the vehicle can be guaranteed if the sum of the destabilizing moment is compensated during a lateral manoeuvre.

Several schemes concerned with the possible active intervention into vehicle dynamics have been proposed. These approaches employ active anti-roll bars, active steering, active braking, active suspensions, or a combination of them (Gaspar et al., 2004). The active anti-roll bar system is the most common method used to improve the roll stability of heavy vehicles. Several control design problems for active anti-roll bar systems have been investigated with many different approaches during the last decades. In (Gaspar et al., 2005a) the authors presented Linear Parameter Varying (LPV) techniques to control the active anti-roll bars, combined with an active brake control on single unit heavy vehicles. The forward velocity is considered as the varying parameter. Other works concerning the yaw-roll model on single unit heavy vehicles have dealt with optimal control (Sampson and Cebon, 2003a), robust control (Vu et al., 2016b), and neural network control (Boada et al., 2007).

The H_∞ control design approach is an efficient tool for improving the performance of a closed-loop system in pre-defined frequency ranges. The key step of the H_∞ control design is the selection of weighting functions which depends on the engineer skill and experience (Skogestad and Postlethwaite, 2003). In many real applications, the difficulty in choosing the weighting functions still increases significantly because the performance specification is not accurately defined i.e., it is simply to achieve

the best possible performance (optimal design) or to achieve an optimally joint improvement of more than one objective (multi-objectives design). So the optimization of weighting functions to satisfy all the desired performances is still an interesting problem. In (Hu et al., 2000) the authors proposed to consider each system, no matter how complex it is, as a combination of sub-systems of the first and second order, for which it is easy to find the good weighting functions to be used in the H_∞ control methodology. However, there is no explicit method to find these functions in the general case. The usual way is to proceed by trial-and-error. Recently, the idea to use an optimization tool was proposed in (Alfaro-Cid et al., 2008). The choice of GAs seems natural because their formulation is well suited for this type of problems (Do et al., 2011).

Based on the integrated model presented in (Vu et al., 2016a), this paper proposes an H_∞ control for active anti-roll bar, the GAs method is used to solve the Multi-Criteria Optimization (MCO) problem for the H_∞ synthesis. The latter work is here extended providing two new main contributions:

- We design here an H_∞ controller for active anti-roll bar system on the integrated model for the single unit heavy vehicle. The aim is to improve the roll stability of the heavy vehicle. The normalized load transfers and the limitation of the input currents generated by the controllers are considered.
- The GAs method is applied to define the weighting functions of the H_∞ controller for the active anti-roll bar system on the integrated model. Thanks to GAs, the conflicting objectives between the normalized load transfers and the input currents are handled using only one single high level parameter.

This paper is organised as follows: Section 2 gives the integrated model for a single unit heavy vehicle. Section 3 presents the MCO problem of active anti-roll bar control. Section 4 illustrates the H_∞ robust control synthesis to improve roll stability of heavy vehicles. In section 5, GAs method is used for MCO

in the H_∞ anti-roll bar control. Section 6 shows the simulation results in the frequency and time domains. Finally, some conclusions are drawn in section 7.

2. INTEGRATED MODEL FOR HEAVY VEHICLES

The proposed integrated model includes four Electronic Servo-Valve Hydraulic (ESHV) actuators (two at the front axle and two at the rear axle) in a linear single unit heavy vehicle yaw-roll model (Gaspar et al., 2005b). The control signal is the electrical current u opening the electronic servo-valve, the output is the force F_{act} generated by the hydraulic actuator. The symbols of the integrated model are found in Table 1.

In the linear single unit heavy vehicle yaw-roll model, the differential equations of motion, i.e., the lateral dynamics, the yaw moment, the roll moment of the sprung mass, the roll moment of the front and the rear unsprung masses, are formalized in the equations (1):

$$\left\{ \begin{array}{l} mv(\dot{\beta} + \dot{\psi}) - m_s h \ddot{\phi} = F_{yf} + F_{yr} \\ -I_{xz} \ddot{\phi} + I_{zz} \ddot{\psi} = F_{yf} l_f - F_{yr} l_r \\ (I_{xx} + m_s h^2) \ddot{\phi} - I_{xz} \ddot{\psi} = m_s g h \phi + m_s v h (\dot{\beta} + \dot{\psi}) \\ \quad - k_f (\phi - \phi_{tf}) - b_f (\dot{\phi} - \dot{\phi}_{tf}) + M_{ARf} + T_f \\ \quad - k_r (\phi - \phi_{tr}) - b_r (\dot{\phi} - \dot{\phi}_{tr}) + M_{ARr} + T_r \\ -r F_{yf} = m_{uf} v (r - h_{uf}) (\dot{\beta} + \dot{\psi}) + m_{uf} g h_{uf} \phi_{tf} - k_{tf} \phi_{tf} \\ \quad + k_f (\phi - \phi_{tf}) + b_f (\dot{\phi} - \dot{\phi}_{tf}) + M_{ARf} + T_f \\ -r F_{yr} = m_{ur} v (r - h_{ur}) (\dot{\beta} + \dot{\psi}) - m_{ur} g h_{ur} \phi_{tr} - k_{tr} \phi_{tr} \\ \quad + k_r (\phi - \phi_{tr}) + b_r (\dot{\phi} - \dot{\phi}_{tr}) + M_{ARr} + T_r \end{array} \right. \quad (1)$$

In (1) the lateral tyre forces $F_{y,i}$ in the direction of velocity at the wheel ground contact points are modelled by a linear stiffness as:

$$\left\{ \begin{array}{l} F_{yf} = \mu C_f \alpha_f \\ F_{yr} = \mu C_r \alpha_r \end{array} \right. \quad (2)$$

with tyre side slip angles:

$$\left\{ \begin{array}{l} \alpha_f = -\beta + \delta_f - \frac{l_f \dot{\psi}}{v} \\ \alpha_r = -\beta + \frac{l_r \dot{\psi}}{v} \end{array} \right. \quad (3)$$

The moment of passive anti-roll bar impacts the unsprung and sprung masses at the front and rear axles as follows:

$$\left\{ \begin{array}{l} M_{ARf} = 4k_{AOf} \frac{t_A t_B}{c^2} \phi - 4k_{AOf} \frac{t_A^2}{c^2} \phi_{uf} \\ M_{ARr} = 4k_{AOr} \frac{t_A t_B}{c^2} \phi - 4k_{AOr} \frac{t_A^2}{c^2} \phi_{ur} \end{array} \right. \quad (4)$$

where k_{AOf} , k_{AOr} are respectively the torsional stiffnesses of the anti-roll bar at the front and rear axles, t_A is half the distance of the two suspensions, t_B is half the distance of the chassis, c is the length of the anti-roll bars' arm.

The torque generated by the active anti-roll bar system at the front axle is now determined by:

$$T_f = 2l_{act} F_{actf} = 2l_{act} A_p \Delta P_f \quad (5)$$

and the torque generated by the active anti-roll bar system at the rear axle is:

$$T_r = 2l_{act} F_{actr} = 2l_{act} A_p \Delta P_r \quad (6)$$

where ΔP_f and ΔP_r are respectively the difference of pressure of the hydraulic actuator at the front and rear axles.

The equations of these electronic servo-valve actuators are given by (7):

Table 1. Symbols of the integrated model (see Gaspar et al. (2005a), Vu et al. (2016a)).

| Symbols | Description |
|---------------|--|
| m_s | Sprung mass |
| $m_{uf,r}$ | Unsprung mass on the front/rear axle |
| m | The total vehicle mass |
| v | Forward velocity |
| h | Height of sprung mass from roll axis |
| $h_{u,i}$ | Height of unsprung mass from ground |
| r | Height of roll axis from ground |
| a_y | Lateral acceleration |
| β | Side-slip angle at center of mass |
| ψ | Heading angle |
| $\dot{\psi}$ | Yaw rate |
| α | Side slip angle |
| ϕ | Sprung mass roll angle |
| $\phi_{uf,r}$ | Unsprung mass roll angle at the front/rear axle |
| δ_f | Steering angle |
| $u_{f,r}$ | Control current at the front/rear axle |
| $C_{f,r}$ | Tire cornering stiffness on the front/rear axle |
| $k_{f,r}$ | Suspension roll stiffness on the front/rear axle |
| $b_{f,r}$ | Suspension roll damping on the front/rear axle |
| $k_{t,f,r}$ | Tire roll stiffness on the front/rear axle |
| I_{xx} | Roll moment of inertia of sprung mass |
| I_{xz} | Yaw-roll inertial of sprung mass |
| I_{zz} | Yaw moment of inertia of sprung mass |
| $l_{f,r}$ | Length of the front axle/rear axle from the CG |
| l_w | Half of the vehicle width |
| μ | Road adhesion coefficient |
| A_p | Area of the piston |
| K_x | Valve flow gain coefficient |
| K_p | Total flow pressure coefficient |
| C_{lp} | Total leakage coefficient |
| V_t | Total volume of trapped oil |
| β_e | Effective bulk modulus of the oil |
| τ | Time constant of the servo-valve |
| K_v | Servo-valve gain |
| $X_{v,f,r}$ | Spool valve displacements at the front/rear axle |

$$\left\{ \begin{array}{l} \frac{V_t}{4\beta_e} \dot{\Delta P}_f + (K_p + C_{lp}) \Delta P_f - K_x X_{vf} \\ \quad + A_p l_{act} \dot{\phi} - A_p l_{act} \dot{\phi}_{uf} = 0 \\ \dot{X}_{vf} + \frac{1}{\tau} X_{vf} - \frac{K_v}{\tau} u_f = 0 \\ \frac{V_t}{4\beta_e} \dot{\Delta P}_r + (K_p + C_{lp}) \Delta P_r - K_x X_{vr} \\ \quad + A_p l_{act} \dot{\phi} - A_p l_{act} \dot{\phi}_{ur} = 0 \\ \dot{X}_{vr} + \frac{1}{\tau} X_{vr} - \frac{K_v}{\tau} u_r = 0 \end{array} \right. \quad (7)$$

Defining the state vector:

$$x = [\beta \ \dot{\psi} \ \phi \ \dot{\phi} \ \phi_{uf} \ \phi_{ur} \ \Delta P_f \ X_{vf} \ \Delta P_r \ X_{vr}]^T$$

The motion differential equations (1)-(7) can be rewritten in the LTI state-space representation as:

$$\left\{ \begin{array}{l} \dot{x} = A \cdot x + B_1 \cdot w + B_2 \cdot u \\ z = C \cdot x + D_1 \cdot w + D_2 \cdot u \end{array} \right. \quad (8)$$

where A , B_1 , B_2 , C , D_1 , D_2 are the model matrices of appropriate dimensions.

The exogenous disturbance (steering angle) is:

$$w = [\delta_f]^T$$

and the control inputs (input currents):

$$u = [u_f \ u_r]^T$$

3. MULTI-CRITERIA OPTIMIZATION OF ACTIVE ANTI-ROLL BAR CONTROL

3.1 Multi-criteria optimization and Pareto-optimal solutions

Multi-Criteria Optimization (MCO) can be described in mathematical terms as follows (Ehrgott, 2005):

$$\min_{x \in S} F(x) = [f_1(x), f_2(x), \dots, f_n(x)] \quad (9)$$

where $n > 1$ and S is the set of constraints defined above. The space in which the objective vector belongs is called the objective space, and the image of the feasible set under F is called the attained set. In the following such a set will be denoted by $C = \{y \in \mathbb{R}^n : y = f(x), x \in S\}$. The scalar concept of optimality does not apply directly in the multi-criteria setting. Here the notion of Pareto optimality is introduced. Essentially, a vector $x^* \in S$ is said to be Pareto optimal for a multi-criteria problem if all other vectors $x \in S$ do not have a higher value for at least one of the objective functions f_i , with $i = 1, \dots, n$, or have the same value for all the objective functions.

There are many formulations to solve the problem (9) such as weighted min-max method, weighted global criterion method, goal programming methods... (Marler and Arora, 2004) and references therein. Here, one uses a particular case of the weighted sum method, where the multi-criteria functions vector F is replaced by the convex combination of objectives:

$$\min_{x \in S} J = \sum_{i=1}^n \alpha_i f_i(x), \quad \sum_{i=1}^n \alpha_i = 1 \quad (10)$$

The vector $\alpha = (\alpha_1, \alpha_2, \dots, \alpha_n)$ represents the gradient of function J . By using various sets of α , one can generate several points in the Pareto set.

The shape of the Pareto surface indicates the nature of the trade-off between the different objective functions. An example of a Pareto curve is reported in Fig 1, where all the points between $(f_2(\hat{x}), f_1(\hat{x}))$ and $(f_2(\bar{x}), f_1(\bar{x}))$ define the Pareto front. These points are called non-inferior points.

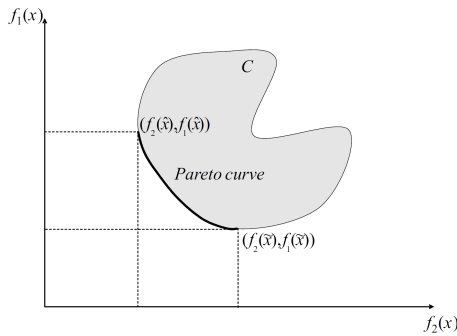


Fig. 1. Example of a Pareto curve.

3.2 Control objective, and MCO for H_∞ active anti-roll bar control

The main objective of the active anti-roll bar control system is to maximize the roll stability of the vehicle to prevent a rollover phenomenon in an emergency. Two main criteria are commonly used to assess the roll stability of the heavy vehicle:

- The normalized load transfer $R_{f,r}$ at the two axles, defined as follows (Hsun-Hsuan et al., 2012):

$$R_f = \frac{\Delta F_{zf}}{F_{zf}}, \quad R_r = \frac{\Delta F_{zr}}{F_{zr}} \quad (11)$$

where F_{zf} is the total axle load at front axle and F_{zr} at rear axle. ΔF_{zf} and ΔF_{zr} are respectively the lateral load transfers at the front and rear axles, which can be given by:

$$\Delta F_{zf} = \frac{k_{uf}\phi_{uf}}{l_w}, \quad \Delta F_{zr} = \frac{k_{ur}\phi_{ur}}{l_w} \quad (12)$$

where k_{uf} and k_{ur} are the stiffness of the tyres, ϕ_{uf} and ϕ_{ur} are the roll angles of the unsprung masses at the front and rear axles, l_w the half of the vehicle's width.

The normalized load transfer $R_{f,r} = \pm 1$ value corresponds to the largest possible load transfers. The roll stability is achieved by limiting the normalized load transfers within the levels corresponding to wheel lift-off.

- The roll angles between the sprung and unsprung masses ($\phi - \phi_u$), give the maximum stabilizing moment of the active anti-roll bar system to be increased. They should stay within the limits of the suspension travel $7 - 8deg$ (Sampson and Cebon, 2003b).

As mentioned above, the objective of the active anti-roll bar control system is to improve the roll stability of heavy vehicles. However, such a performance objective must be balanced with the energy consumption of the anti-roll bar system due to the input current entering the electronic servo-valve of the actuators. Therefore the objective function is selected as follows:

$$f = \alpha f_{Normalized-load-transfer} + (1 - \alpha) f_{Control-cost} \quad (13)$$

The vector $\alpha = [0 \div 1]$ is the gradient of function f . When α moves to 0, the optimal problem focusses on minimizing input currents. And conversely, when α moves to 1, the optimal problem focusses on minimizing normalized load transfers.

In the objective function (13), $f_{Normalized-load-transfer}$ and $f_{Control-cost}$ are performance indices corresponding to the normalized load transfers and input currents at the two axles, which are defined as follows:

$$\begin{cases} f_{Normalized-load-transfer} = \frac{1}{2} \left(\sqrt{\frac{1}{T} \int_0^T R_f^2(t) dt} + \sqrt{\frac{1}{T} \int_0^T R_r^2(t) dt} \right) \\ f_{Control-cost} = \frac{1}{2} \left(\frac{\sqrt{\frac{1}{T} \int_0^T u_f^2(t) dt}}{\sqrt{\frac{1}{T} \int_0^T u_f^2(t)_{max} dt}} + \frac{\sqrt{\frac{1}{T} \int_0^T u_r^2(t) dt}}{\sqrt{\frac{1}{T} \int_0^T u_r^2(t)_{max} dt}} \right) \end{cases} \quad (14)$$

where $u_{f,rmax}$ are defined when the optimal problem focusses only on the normalized load transfers (i.e., the input currents are then not considered in the optimisation problem). In that case, $\alpha = 1$ and $f = f_{Normalized-load-transfer}$.

The MCO problem represented by the equation (13) can not be resolved directly in the synthesis of H_∞ controller. Thus, summarizing the implementation is done in this paper is described as Fig 2. The generalized plant includes the integrated model (section 2) and the weighting functions. The controller is synthesised in term of H_∞ method (section 4). The conflicting objective between roll stability and energy consumption is the computation of the close-loop performance (MCO problem in section 3). Depending on the purpose of the MCO problem, the weighting functions are appropriately selected by GAs (section 5). The optimal parameters obtained from GAs are sent to the weighting functions to calculate the characteristics of the closed-loop system (section 6).

4. H_∞ ACTIVE ANTI-ROLL BAR CONTROL TO IMPROVE ROLL STABILITY OF HEAVY VEHICLES

4.1 Background on H_∞ control

The interested reader may refer to (Skogestad and Postlethwaite, 2003), (Scherer and Weiland, 2005) for detailed explanations on H_∞ control design.

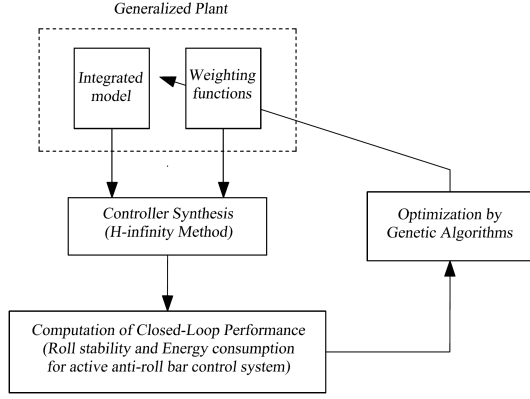


Fig. 2. Controller optimization for H_∞ active anti-roll bar using Genetic Algorithms.

The H_∞ control problem is formulated according to the generalized control structure shown in Fig 3.

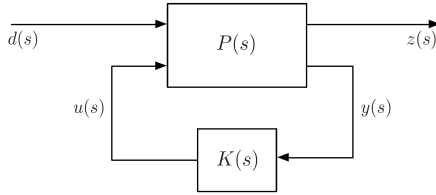


Fig. 3. Generalized control structure.

with P partitioned as

$$\begin{bmatrix} z \\ y \end{bmatrix} = \begin{bmatrix} P_{11}(s) & P_{12}(s) \\ P_{21}(s) & P_{22}(s) \end{bmatrix} \begin{bmatrix} d \\ u \end{bmatrix} \quad (15)$$

and

$$u = K(s).y \quad (16)$$

which yields

$$\frac{z}{d} = \mathcal{F}_l(P, K) := [P_{11} + P_{12}K[I - P_{22}K]^{-1}P_{21}] \quad (17)$$

The aim is to design a controller $K(s)$ that reduces the signal transmission path from disturbances d to performance outputs z and also stabilizes the closed-loop system. The H_∞ problem is to find K which minimizes γ such that

$$\|\mathcal{F}_l(P, K)\|_\infty < \gamma \quad (18)$$

By minimizing a suitably weighted version of (18), the control aim is achieved, as presented below.

4.2 H_∞ control design for active anti-roll bar system

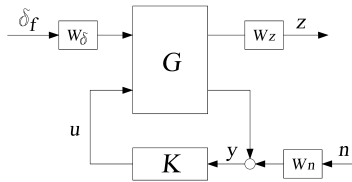


Fig. 4. Closed-loop structure of an H_∞ active anti-roll bar control.

Figure 4 shows the closed-loop structure of an H_∞ control designed for the active anti-roll bar system on a single unit heavy vehicle, using ESVH actuators. In the diagram, the feedback structure includes the nominal model G , the controller K , the performance output z , the control input u , the measured

output y , the measurement noise n . The steering angle δ_f is the disturbance signal, which is set by the driver. The weighting functions W_δ, W_z, W_n are presented below.

According to Figure 4, the concatenation of the linear model (8) with the performance weighting functions lead to the state space representation of $P(s)$:

$$\begin{bmatrix} \dot{x} \\ z \\ y \end{bmatrix} = \begin{bmatrix} A & B_1 & B_2 \\ C_1 & D_{11} & D_{12} \\ C_2 & D_{21} & D_{22} \end{bmatrix} \begin{bmatrix} x \\ w \\ u \end{bmatrix} \quad (19)$$

with the exogenous input:

$$w = \begin{bmatrix} \delta_f & n \end{bmatrix}$$

the control input:

$$u = \begin{bmatrix} u_f & u_r \end{bmatrix}^T$$

where u_f and u_r are the input current at the two axles.

the performance output vector:

$$z = \begin{bmatrix} u_f & u_r & R_f & R_r & a_y \end{bmatrix}^T$$

and the measured output vector:

$$y = \begin{bmatrix} a_y & \dot{\phi} \end{bmatrix}^T$$

The input scaling weight W_δ normalizes the steering angle to the maximum expected command. It is selected as $W_\delta = \pi/180$, which corresponds to a 1° steering angle command.

The weighting function W_n is selected as a diagonal matrix, which accounts for small sensor noise models in the control design. The noise weights are chosen as $0.01(m/s^2)$ for the lateral acceleration and $0.01(^0/sec)$ for the derivative of roll angle $\dot{\phi}$ (Gaspar et al., 2004).

The weighting functions matrix W_z represents the performance output, $W_z = \text{diag}[W_{zu}, W_{zR}, W_{za}]$. The purpose of the weighting functions is to keep the control inputs, normalized load transfers and lateral acceleration as small as possible over the desired frequency range. These weighting functions can be considered as penalty functions, that is, weights should be large in the frequency range where small signals are desired and small where larger performance outputs can be tolerated.

The weighting function W_{zu} is chosen as $W_{zu} = \text{diag}[W_{zuf}, W_{zur}]$, corresponding to the input currents at the front and rear axles, and are chosen as:

$$W_{zuf} = \frac{1}{Z_1}; \quad W_{zur} = \frac{1}{Z_2} \quad (20)$$

The weighting function W_{zR} is chosen as $W_{zR} = \text{diag}[W_{zRf}, W_{zRr}]$, corresponding to the normalized load transfers at front and rear axles, and are selected as:

$$W_{zRf} = \frac{1}{Z_3}; \quad W_{zRr} = \frac{1}{Z_4} \quad (21)$$

The weighting function W_{za} is selected as:

$$W_{za} = Z_{51} \frac{Z_{52}s + Z_{53}}{Z_{54}s + Z_{55}} \quad (22)$$

Here, the weighting function W_{za} corresponds to a design that avoids the rollover situation with the bandwidth of the driver in the frequency range up to more than $4rad/s$. This weighting function will directly minimize the lateral acceleration when it reaches the critical value, to avoid the rollover.

As said before, the key step of the H_∞ control design is how to select the weighting function. This is not an easy task even with good engineers, because it depends on the engineer skill and experience. From equations (20) - (22), Z_i and $Z_{5,j}$ are constant parameters. The following variables are to be defined: $Z_1, Z_2, Z_3, Z_4, Z_{51}, Z_{52}, Z_{53}, Z_{54}, Z_{55}$. In the next section, the

GAs method will be used to find these variables, suited for the MCO problem.

5. USING GENETIC ALGORITHMS FOR MULTI-CRITERIA OPTIMIZATION IN H_∞ ANTI-ROLL BAR CONTROL

This section introduces the MCO problem for the H_∞ active anti-roll bar control on heavy vehicles, which is solved by using the GAs method.

5.1 Genetic Algorithms

A Genetic Algorithms developed by J.H. Holland (Holland, 1975) is a model of machine learning, which derives its behavior from a metaphor of the processes of evolution in nature. GAs are executed iteratively on a set of coded chromosomes, called a population, with three basic genetic operation: selection, crossover and mutation. Each member of the population, called a chromosome (or individual) is represented by a string. GAs use only the objective function information and probabilistic transition rules for genetic operations. The primary operation of GAs is the crossover. The crossover happens with a probability of 0.9 and the mutation happens with a small probability 0.095. The basic flowchart of GAs is shown in Fig 5.

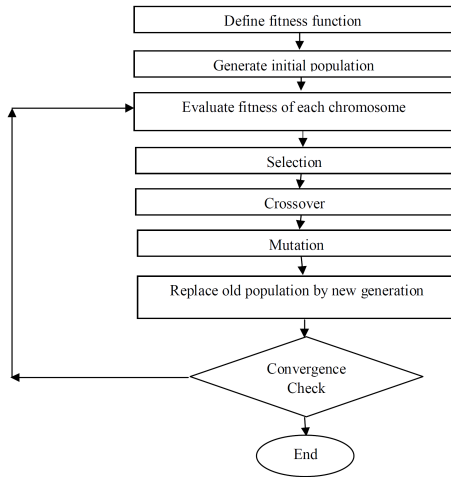


Fig. 5. Basic flowchart of Genetic Algorithm.

5.2 Solving multi-criteria optimization by genetic algorithms

From the objective function in (13), the MCO problem for the H_∞ active anti-roll bar control can be defined as:

$$\min_{p \in P} F(p), F(p) := [f_{\text{Normalized-load-transfer}}, f_{\text{Control-cost}}]^T \quad (23)$$

$$P := \{p = [Z_1, Z_2, Z_3, Z_4, Z_{51}, Z_{52}, Z_{53}, Z_{54}, Z_{55}]^T \in R \mid p^l \leq p \leq p^u\}$$

where $F(p)$ is the vector of objectives, p denotes the vector of the weighting function parameters, and p^l , p^u represent the lower and upper bounds of the weighting function selection. The lower and upper bounds of the weighting function parameters are given in Table 2. Besides the minimization of the objective function from equations (13) and (23), we also have to account for the limitations of the normalized load transfers, roll angle of suspensions, as well as the input currents at each axle. These limitations are considered as the optimal conditions (binding conditions) shown in the Table 3.

The proposed weighting function optimization procedure for the H_∞ active anti-roll bar control synthesis is as follows:

Table 2. Lower and upper bounds of the weighting functions.

| Bounds | W_{2uf} | W_{2ur} | W_{2rf} | W_{2rr} | W_{2a} | | | | |
|-------------|-----------|-----------|-----------|-----------|----------|------------------|----------|----------|----------|
| | Z_1 | Z_2 | Z_3 | Z_4 | Z_{51} | Z_{52} | Z_{53} | Z_{54} | Z_{55} |
| Lower bound | 0.001 | 0.001 | 0.1 | 0.1 | 0.5 | $\frac{1}{3000}$ | 1 | 10 | 0.001 |
| Upper bound | 10 | 10 | 100 | 100 | 100 | 10 | 900 | 1000 | 20 |

Table 3. Binding conditions.

| No | Note | Maximum value | Unit |
|----|----------------------|---------------|------|
| 1 | $ \phi - \phi_{uf} $ | < 7 | deg |
| 2 | $ \phi - \phi_{ur} $ | < 7 | deg |
| 3 | $ R_f $ | < 1 | - |
| 4 | $ R_r $ | < 1 | - |
| 5 | $ u_f $ | < 20 | mA |
| 6 | $ u_r $ | < 20 | mA |

- **Step 1:** Initialize with the weighting functions (it depends on the engineer skill and experience), the vector of weighting functions selected as $p = p_0$.
- **Step 2:** Select lower bound, upper bound, scaling factor, offset and start point.
- **Step 3:** Format optimal algorithm, select the vector of objectives with the variation of switch value from 0 to 1 and then solve the minimization problem.
- **Step 4:** Select the individuals, apply crossover and mutation to generate a new generation: $p = p_{new}$.
- **Step 5:** Evaluate the new generation by comparing with the binding conditions. If the criteria of interest are not satisfied, go to step 3 with $p = p_{new}$; else, stop and save the best individual: $p_{opt} = p_{new}$.

6. SIMULATION RESULTS

6.1 Optimization results

Thanks to the GAs method, Table 4 gives a synthesis of the values of the variables Z_i , Z_{5j} in six cases for $\alpha = [0; 0.25; 0.5; 0.7; 0.9; 1]$, as explained in (13). When $\alpha = 0$, $f = f_{\text{Control-cost}}$, the optimal problem focusses only on the input currents and when $\alpha = 1$, $f = f_{\text{Normalized-load-transfer}}$, the optimal problem focusses only on the normalized load transfers. Figure 6 shows the conflicting relation between the normalized load transfers and control costs with some Pareto-optimal points, computed for the H_∞ active anti-roll bar on heavy vehicles. They are generated for different values of α in the range of $[0; 1]$.

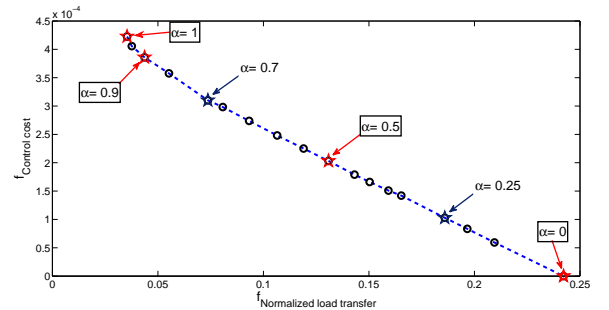


Fig. 6. The Pareto frontier for the active anti-roll bar on heavy vehicles using ESVH actuators.

To evaluate the optimization procedure, the simulation results in both frequency and time domains are done and compared for five cases: passive anti-roll bar (Vu et al., 2016a) and H_∞ active anti-roll bar with $\alpha = [0; 0.5; 0.9; 1]$.

Table 4. Optimization results for the weighting functions of H_∞ active anti-roll bar.

| Controllers | W_{zurf} | W_{zur} | W_{zRf} | W_{zRr} | W_{za} | | | | |
|-----------------|------------|-----------|-----------|-----------|----------|----------|----------|----------|----------|
| | Z_1 | Z_2 | Z_3 | Z_4 | Z_{51} | Z_{52} | Z_{53} | Z_{54} | Z_{55} |
| $\alpha = 0$ | 0.060 | 0.020 | 0.100 | 0.965 | 0.673 | 0.948 | 1.063 | 972.212 | 0.855 |
| $\alpha = 0.25$ | 0.057 | 0.052 | 0.51 | 0.863 | 0.863 | 0.664 | 155.627 | 651.707 | 0.573 |
| $\alpha = 0.5$ | 0.099 | 0.0773 | 1.403 | 0.217 | 0.812 | 0.813 | 88.666 | 407.658 | 1.001 |
| $\alpha = 0.7$ | 0.057 | 0.066 | 0.412 | 0.221 | 0.832 | 0.514 | 139.609 | 357.401 | 1.901 |
| $\alpha = 0.9$ | 0.066 | 0.072 | 0.616 | 0.482 | 0.724 | 0.492 | 202.316 | 455.747 | 0.544 |
| $\alpha = 1$ | 0.07 | 0.090 | 0.655 | 0.305 | 0.545 | 0.245 | 444.397 | 839.299 | 0.163 |

6.2 Evaluation of optimization results in frequency domain

In this section, the frequency response of the heavy vehicle is shown in the nominal parameters case of the single unit heavy vehicle being considered, characterized by the forward velocity V at 70Km/h and the road adhesion coefficient $\mu = 1$ (see, Gaspar et al. (2004) and Vu et al. (2016a)). Figures 7 and 8 show the transfer function magnitude of the normalized load transfers at the two axles $\frac{R_{f,r}}{\delta_f}$.

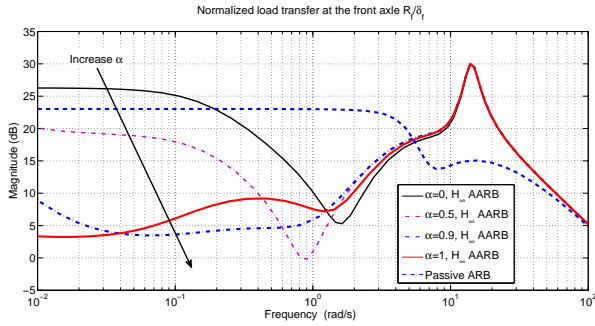


Fig. 7. Transfer function magnitude of the normalized load transfer at the front axle $\frac{R_f}{\delta_f}$.

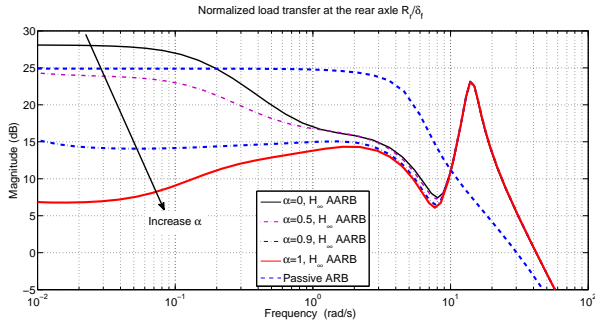


Fig. 8. Transfer function magnitude of the normalized load transfer at the rear axle $\frac{R_r}{\delta_f}$.

To assess the roll stability of the heavy vehicle using the four H_∞ active anti-roll bar controllers. The reduction of the magnitude of transfer functions compared with the passive anti-roll bar case is considered at 10^{-2}rad/s and at 2rad/s as:

$$\lambda(X) = \frac{X_{\text{active}}}{\delta_f} - \frac{X_{\text{passive}}}{\delta_f} \quad (24)$$

where X is the variable of interest, which are the normalized load transfers $R_{f,r}$.

Figure 9 shows the reduction of the magnitude of transfer functions of the normalized load transfer compared with the passive anti-roll bar case at 10^{-2}rad/s and at 2rad/s . We can

see that at 10^{-2}rad/s the controller with $\alpha = 0$ decreases the roll stability, meanwhile, when the value of α increases, the roll stability of the heavy vehicle increases. The curves are very different. At 2rad/s the transfer functions are not so different. This will be explained in further studies.

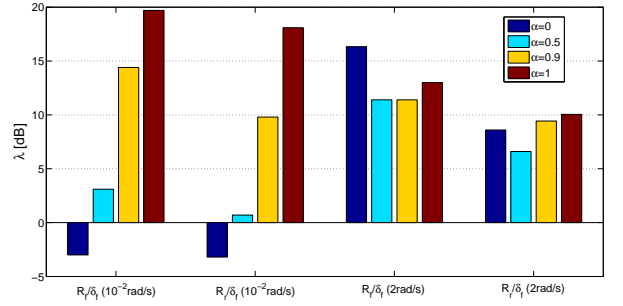


Fig. 9. Reduction of the magnitude of transfer functions of the normalized load transfers at the two axles compared with the passive anti-roll bar case (see (24)).

Figures 10 and 11 show the transfer function magnitude of the input currents at the two axles $\frac{u_{f,r}}{\delta_f}$: when α increases (the MCO problem focusses on the minimizing the normalized load transfers), the total input currents also increase. It's proven for the normalized load transfer and the input current that they are two conflicting performance objectives.

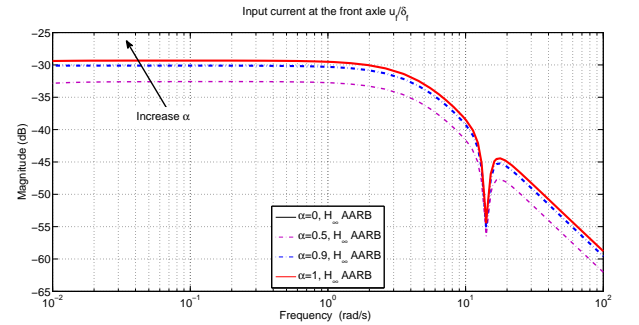


Fig. 10. Transfer function magnitude of the input current at the front axle $\frac{u_f}{\delta_f}$.

Thus through the MCO problem, we can choose the weighting functions to enhance the roll stability of the heavy vehicle in the low frequency range as well as in the high frequency range up to over 4rad/s which is the limited bandwidth of the driver (Gaspar et al., 2004).

6.3 Evaluation of optimization results in time domain

In this section, the cornering responses of a single unit vehicle can be seen. The steering angle (disturbance) applied in the simulation is a step signal as in Fig 12.

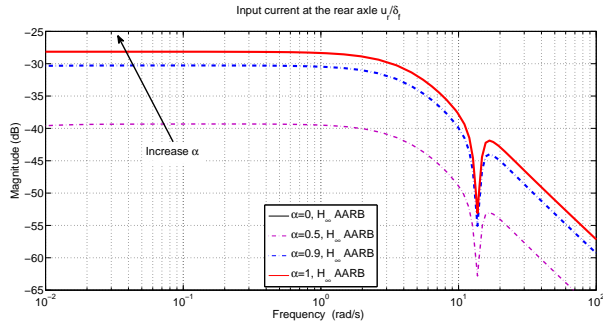


Fig. 11. Transfer function magnitude of the input current at the rear axle $\frac{u_r}{\delta_f}$.

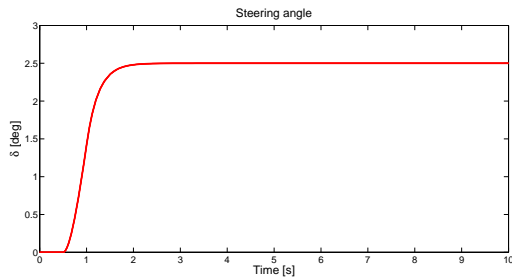


Fig. 12. Steering angle in the cornering manoeuvre (Gaspar et al., 2004).

The forward velocity of the heavy vehicle continuously varies during operation, especially in the case of an emergency. The rollover of the heavy vehicle often occurs with a forward velocity within 60 to 110Km/h. In Figures 13 - 14 we consider the forward velocity of the heavy vehicle up to 160Km/h in order to evaluate the roll stability when the normalized load transfers reach its limitations.

From Figure 13, we can see that the maximum absolute value of normalized load transfers at the front axle reaches the limit “1” in the case of $\alpha = [0; 0.5; 0.9; 1]$ where the forward velocities are respectively 74, 110, 139, 144Km/h. Note that in the case of the passive anti-roll bar, we get 92Km/h for the forward velocity.

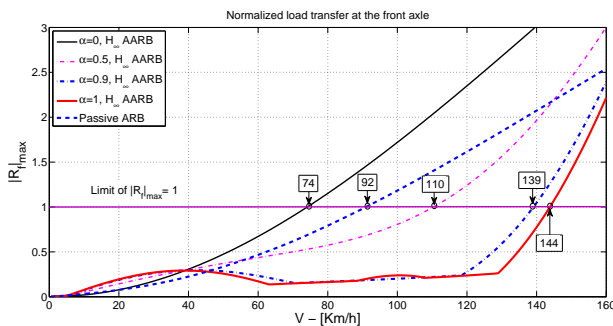


Fig. 13. Effect of the forward velocity on the normalized load transfer: front axle R_f .

Considering Figure 14, the maximum absolute value of the normalized load transfers at the rear axle reaches the limit “1” in the case of $\alpha = [0; 0.5; 0.9; 1]$ where the forward velocities are respectively 66, 84, 129, 139Km/h. Note that in the case of the passive anti-roll bar, we get 80Km/h for the forward velocity. From Figures above, we can conclude that the risk of the

rollover of heavy vehicles is reduced thanks to the multi objective H_∞ controller.

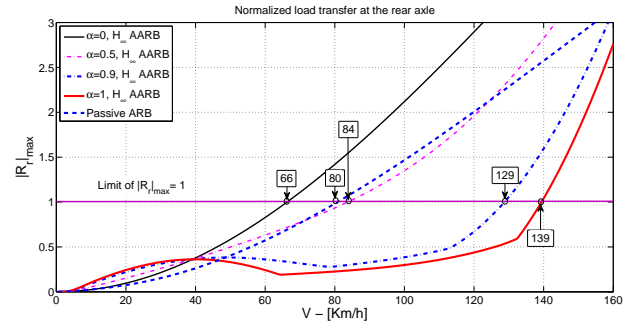


Fig. 14. Effect of the forward velocity on the normalized load transfer: rear axle R_r .

7. CONCLUSION

In this paper, the integrated model of a single unit heavy vehicle including four ESVH actuators is used to develop a linear H_∞ control scheme maximizing its roll stability in order to prevent rollover. The normalized load transfers and the limitations of the input currents are considered in the development.

A weighting function optimization procedure using GAs for H_∞ active anti-roll bar control on the integrated model has also been proposed. The conflicting objectives between the normalized load transfers and input currents are handled using only one high level parameter, which is a great advantage to solve the multi-objective control problem. The simulation results in frequency and time domains have shown the efficiency of GAs in finding a suitable controller to satisfy the MCO problem.

Even if a LTI controller seems to performs reasonably well here, the comparison with an LPV controller (scheduled by the vehicle velocity) will be of interest for future works.

REFERENCES

- Alfaro-Cid, E., McGookin, E., and Murray-Smith, D. (2008). Optimisation of the weighting functions of an H_∞ controller using genetic algorithms and structured genetic algorithms. *International Journal of Systems Science*, 39(4), 335–347.
- Boada, M., Boada, B., Quesada, A., Gaucha, A., and Daz, V. (2007). Active roll control using reinforcement learning for a single unit heavy vehicle. In *12th IFToMM World Congress*. Besancon, France.
- Do, L.A., Sename, O., Dugard, L., and Boussaad, S. (2011). Multi-objective optimization by genetic algorithms in H_∞/LPV control of semi-active suspension. In *IFAC World Congress - 18th IFAC WC 2011*. Italy.
- Ehrgott, M. (2005). *Multicriteria optimization*. Springer, 2nd edition.
- Gaspar, P., Bokor, J., and Szaszi, I. (2004). The design of a combined control structure to prevent the rollover of heavy vehicles. *European Journal of Control*, 10(2), 148–162.
- Gaspar, P., Bokor, J., and Szaszi, I. (2005a). Reconfigurable control structure to prevent the rollover of heavy vehicles. *Control Engineering Practice*, 13(6), 699–711.
- Gaspar, P., Szabo, Z., and Bokor, J. (2005b). The design of an integrated control system in heavy vehicles based on an lpv method. In *Proceedings of the 44th IEEE Conference on Decision and Control, and the European Control Conference*. Seville, Spain.

- Holland, J.H. (1975). *Adaptation in natural and artificial systems: an introductory analysis with applications to biology, control, and artificial intelligence*. Ann Arbor: University of Michigan Press.
- Hsun-Hsuan, H., Rama, K., and Dennis, A.G. (2012). Active roll control for rollover prevention of heavy articulated vehicles with multiple-rollover-index minimisation. *Vehicle System Dynamics: International Journal of Vehicle Mechanics and Mobility*, 50(3), 471–493.
- Hu, J., Bohn, C., and Wu, H. (2000). Systematic H_∞ weighting function selection and its application to the real-time control of a vertical take-off aircraft. *Control Engineering Practice*, 8, 241–252.
- Marler, R. and Arora, J. (2004). Survey of multi-objective optimization methods for engineering. *Structural and Multidisciplinary Optimization*, 26, 369–395.
- Sampson, D. and Cebon, D. (2003a). Achievable roll stability of heavy road vehicles. In *Proceedings of the Institution of Mechanical Engineers, Part D: Journal of Automobile Engineering*, volume 217, 269–287. United Kingdom.
- Sampson, D. and Cebon, D. (2003b). Active roll control of single unit heavy road vehicles. *Vehicle System Dynamics: International Journal of Vehicle Mechanics and Mobility*, 40(4), 229–270.
- Scherer, C. and Weiland, S. (2005). Linear matrix inequalities in control. University Lecture.
- Skogestad, S. and Postlethwaite, I. (2003). *Multivariable Feedback Control*. John Wiley & Sons, 2nd edition.
- Vu, V.T., Sename, O., Dugard, L., and Gaspar, P. (2016a). Active anti-roll bar control using electronic servo-valve hydraulic damper on single unit heavy vehicle. In *IFAC Symposium on Advances in Automotive Control - 8th AAC 2016*. Norrköping, Sweden.
- Vu, V.T., Sename, O., Dugard, L., and Gaspar, P. (2016b). H_∞ active anti-roll bar control to prevent rollover of heavy vehicles: a robustness analysis. In *IFAC Symposium on System Structure and Control - 6th SSSC 2016*. Istanbul, Turkey.